Check for updates

ECOGRAPHY

*Research Article*

# Combining thermal and hydric constraints for spatially predicting the activity suitability of Neotropical Leptodactylid frogs

**Luis M. Senzano**[1], **Milton C. Ribeiro**[2], **Sidney F. Gouveia**[3] **and Denis V. Andrade**[1]

[1]Laboratório de Biologia Experimental e Integrativa, Departamento de Biodiversidade, Universidade Estadual Paulista (UNESP), Rio Claro, SP, Brasil
[2]Laboratório de Ecologia Espacial e Conservação (LEEC), Departamento de Biodiversidade, Universidade Estadual Paulista (UNESP), Rio Claro, SP, Brasil
[3]Laboratório de Pesquisa Integrativa em Biodiversidade, Departamento de Ecologia, Universidade Federal de Sergipe (UFS), São Cristóvão, SE, Brasil

**Correspondence: Luis M. Senzano (lm.senzano@gmail.com)**

**Ecography**
**2026: e07617**
doi: 10.1002/ecog.07617
Subject Editor: Tatsuya Amano
Editor-in-Chief:
Christine N. Meynard
Accepted 19 September 2025

Amphibians balance their thermal and water budgets depending on their physiological state and the physical environment, with both factors capable of constraining activity. Most mechanistic assessments emphasize thermal over water constraints, potentially missing important aspects of amphibian ecophysiological patterns. Here, we evaluate the potential role of thermal and hydric constraints on the activity time of three Neotropical frogs (*Leptodactylus fuscus*, *L. mystacinus*, and *L. macrosternum*) across their geographic distribution. We inferred environmental suitability based on heat and mass transfer principles through a mechanistic modeling procedure anchored to empirically obtained laboratory and field data. We integrated species-specific thermal, hydric, and performance attributes with their immediate physical environment (ground-level microclimate) under nocturnal conditions, while allowing for the interactive response of retreating into shelter when facing physiological heat or water stress. Our results demonstrate the desiccation-prone role of smaller body sizes in increasing hydric restrictions and inhibiting activity, even under thermally adequate conditions, as well as the role of shelters as thermal and hydric refugia. More strikingly, thermal-induced restrictions in activity were linked to low temperatures rather than warmer conditions, indicating that their engagement in activity is mostly driven by the lower thermal bounds of their functional organismal performance. These findings provide a broader picture of climatic constraints on anuran activity and distribution, as well as insights into how species may respond to changing climatic conditions.

Keywords: amphibians, locomotor performance, mechanistic species distribution modeling, microclimate, shelter use

## Introduction

Thermal and hydric constraints are key drivers of ectotherm activity (Kearney 2013, Gunderson and Leal 2016) and several ecological and geographic patterns (Rozen-Rechels et al. 2019). In general, ectotherms engage in activity when ambient conditions

© 2025 The Author(s). Ecography published by John Wiley & Sons Ltd on behalf of Nordic Society Oikos
This is an open access article under the terms of the Creative Commons Attribution License, which permits use, distribution and reproduction in any medium, provided the original work is properly cited.

NORDIC SOCIETY OIKOS
www.ecography.org

allow them to maintain body temperature ($T_b$) within certain thermal thresholds, retreating to refuges if temperature becomes physiologically restricting (Kearney et al. 2018, Huey and Kingsolver 2019). The sensitivity of their performance to changes in $T_b$ is often described using a thermal performance curve (TPC). This curve typically increases from a critical minimum temperature ($CT_{min}$) until it peaks at an optimal temperature ($T_{opt}$) and then decreases until it reaches a critical thermal maximum ($CT_{max}$) (Huey and Stevenson 1979). However, hotter temperatures usually increase the risk of organisms losing excessive water through evaporation from body surfaces, potentially compromising water balance. This particular risk is especially relevant in groups with highly permeable skin, such as the amphibians (Wells 2007), in which excessive evaporative water loss (EWL) may lead to dehydration. In turn, dehydration can impact behavioral performance either directly by its deleterious effects on physiological systems, or indirectly by inducing the lowering in $T_b$ (Köhler et al. 2011). Consequently, it is expected that amphibians integrate their activity within a given range of temperature and humidity levels that provide enough heat to achieve adequate levels of performance while minimizing the risk of dehydration (Seebacher and Alford 2002, Mitchell and Bergmann 2016).

The amphibians' ability to maintain their $T_b$ close to their $T_{opt}$ is indeed constrained by hydration and other competing thermal-dependent physiological demands (Mitchell and Bergmann 2016) or by the availability of suitable habitats (Seebacher and Alford 2002). As microclimatic conditions constantly change, the thermal and hydric states of animals are bound to vary, which, in turn, may impose limits on their engagement in activity (Tracy et al. 2014, Ruthsatz et al. 2022). Restrictions on activity time resulting from thermal or hydric trade-offs potentially lead to reduced food intake, energy deficits, increased reproductive costs (the 'lost opportunity hypothesis'; Huey and Slatkin 1976, Huey and Kingsolver 2019, Cunningham et al. 2021), ultimately leading to local population decline or even extinction (Sinervo et al. 2010, Bestion et al. 2015). Among amphibians from tropical and subtropical regions, where daytime temperatures are higher and more variable than those at night (Schwarzkopf and Alford 1996, Muñoz and Bodensteiner 2019), most species are strictly nocturnal (Anderson and Wiens 2017). Although nocturnality may buffer against the higher water costs usually prevalent during daytime, amphibians are not free from water stress during nighttime. Nocturnality significantly affects amphibian behavioral performance because the reduced evaporative water loss is usually accompanied by decreased thermoregulatory opportunities (Hitchcock and McBrayer 2006, Rock and Cree 2008). Therefore, the compromise with water balance regulation may lead to reduced opportunities to keep $T_b$ close to its optimal function (O'Connor and Tracy 1992), reducing or even entirely restricting the time allocated to activity (Feder and Londos 1984, Peterman and Semlitsch 2014).

These thermal and hydric constraints can compound temporally and spatially, affecting amphibians' niche and geographic distribution (Rubalcaba et al. 2019a). Bridging local activity patterns with broad-scale patterns of environmental constraints is challenging but essential for understanding climatic effects on species' resilience. Mechanistic models are a powerful tool for integrating the particular biophysical and physiological attributes of animals with microclimatic conditions to scale them up to larger geographical extents. Such models have been deployed to investigate amphibian activity based on the potential interactions between thermal and hydric constraints (Enriquez-Urzelai et al. 2019, Rubalcaba et al. 2019a, Ginal et al. 2021, Greenberg and Palen 2021). However, mechanistic assessments focused on Neotropical amphibians are rare, and the few physiological-based studies primarily focus on thermal constraints for activity (Cassemiro et al. 2012, Díaz-Ricaurte et al. 2020). This results in overlooking the potential hydric compromises regarding evaporative water loss during activity (Kearney et al. 2008).

Here, we use thermal and hydric organismal traits from three nocturnal Neotropical frogs (*Leptodactylus fuscus*, *L. mystacinus*, and *L. macrosternum*) and combine multiple modeling approaches to identify potential thermal and hydric constraints on their activity throughout their geographic distribution. We integrated biophysical aspects of the species with physiological information on thermal ($CT_{min}$ and $CT_{max}$), hydric (evaporative water loss and dehydration tolerance; EWL and $EWL_{tol}$), and behavioral performance (thermal performance curves for locomotion) with hourly ground-level microclimate variables (Kearney et al. 2014). Using this spatially explicit biophysical modeling approach (Rubalcaba et al. 2019b), we identified physiologically limiting constraints on activity and inferred environmental optimality in areas potentially accessible to the studied species.

## Material and methods

### Frog species

*Leptodactylus* frogs (Anura, Leptodactylidae) are a morphologically and ecologically diverse genus occupying various habitats throughout the Neotropics, being particularly abundant in lowland and montane tropical forests (Wells 2007). We focused on three leptodactylid frog species: the small-sized *Leptodactylus fuscus* (5–9 g body mass; snout–vent length (SVL) 32–56 mm), the moderate-sized *L. mystacinus* (14–18 g mass; SVL 43–67 mm), and the moderate-to-large-size *L. macrosternum* (55–80 g mass; SVL 65–97 mm) (Sá et al. 2014). Apart from the size, these frogs are generally similar in morphology and natural history. Unlike most treefrogs, which can avoid rapid desiccation due to a diverse set of specializations acting to lower skin permeability (Lillywhite 2006), our *Leptodactylus* species can be considered 'typical' anurans in the sense that they lack specialized integumental features to minimize EWL. Thus, the three *Leptodactylus* species herein studied have low skin resistance to evaporation. They also exhibit ground-dwelling



16000587, 2026, 1, Downloaded from https://nsojournals.onlinelibrary.wiley.com/doi/10.1002/ecog.07617 by Universidade Estadual Paulista, Wiley Online Library on [04/09/2026]. See the Terms and Conditions (https://onlinelibrary.wiley.com/terms-and-conditions) on Wiley Online Library for rules of use; OA articles are governed by the applicable Creative Commons License

nocturnal habits and spend most of their time in highly to moderately moist areas (Solano 1987, Silva and Giaretta 2008). Indeed, they are generally associated with habitats near standing waters. However, *L. fuscus* can occur at greater distances from bodies of water than its congeners during its peak reproductive period, as it constructs foam nests farther from permanent water sources (Méndez-Narváez et al. 2015, Venturelli et al. 2021). Their activity and reproductive periods coincide with the warmest and wettest months of the year (Haddad et al. 2013).

### Physiological data

Physiological information used to perform mechanistic models corresponds to average trait values collected from Leptodactylid frogs (unpubl.). Details of the animal housing conditions and protocols for experimental data collection are virtually the same as those provided elsewhere (Maenaka et al. 2023), but here we describe them briefly. We used adult individuals of both sexes of *L. fuscus* (n = 46; 8.79 ± 1.60 g; 43.12 ± 1.32 mm of SVL), *L. mystacinus* (n = 11; 14.92 ± 1.83 g; 50.55 ± 1.23 mm), and *L. macrosternum* (n = 14; 56.87 ± 8.97 g; 81.52 ± 4.97 mm) collected in São Paulo State, southeastern Brazil. Physiological data comprise critical components of thermal, water balance, and locomotor functions related to ambient constraints and/or parameters necessary as inputs to solve the ectotherm heat model.

We empirically quantified the frogs' behavioral performance by constructing their thermal performance curves (TPC) for the locomotor/escape response. More specifically, we determined the maximum jump distance (out of five consecutive jumps) achieved by the animals at different temperatures, which was then used to construct species-specific TPC. All trials were conducted at night in a 5-m long jumping arena at six test temperatures (10, 15, 20, 25, 30, and 35°C), with individual frogs tested once at each temperature, and no more than one temperature per day (details in the Supporting information). From the TPC, we extracted the frog temperature at which optimal performance was attained ($T_{opt}$) and the thermal performance breadth ($B_{80}$: the range of $T_b$ across which jumping ability remained at least 80% of maximal performance) (Fig. 1). Even though $B_{80}$ represents a performance decrease compared to $T_{opt}$, it is generally interpreted as the thermal range at which animals perform 'well' (Huey and Stevenson 1979). Beyond the $B_{80}$ limits, performance drops toward the critical thermal minimum ($CT_{min}$) or maximum ($CT_{max}$), the physiological endpoints at which performance is zero. The $CT_{min}$ and $CT_{max}$, however, were determined in a different set of experiments independent of TPC determinations. The $CT_{min}$ and $CT_{max}$ were measured by gradually decreasing or increasing $T_b$ at a constant cooling/heating rate (1°C 10 $min^{-1}$) until attaining the non-lethal point of righting reflex loss (a transitory loss of skeletal muscles coordination identified by the animals' incapacity to right their body after being flipped onto their back). Because activity cannot occur beyond these critical limits, we used them as the lower and upper thermal thresholds for activity in our computing simulations. We should note, however, that this may slightly

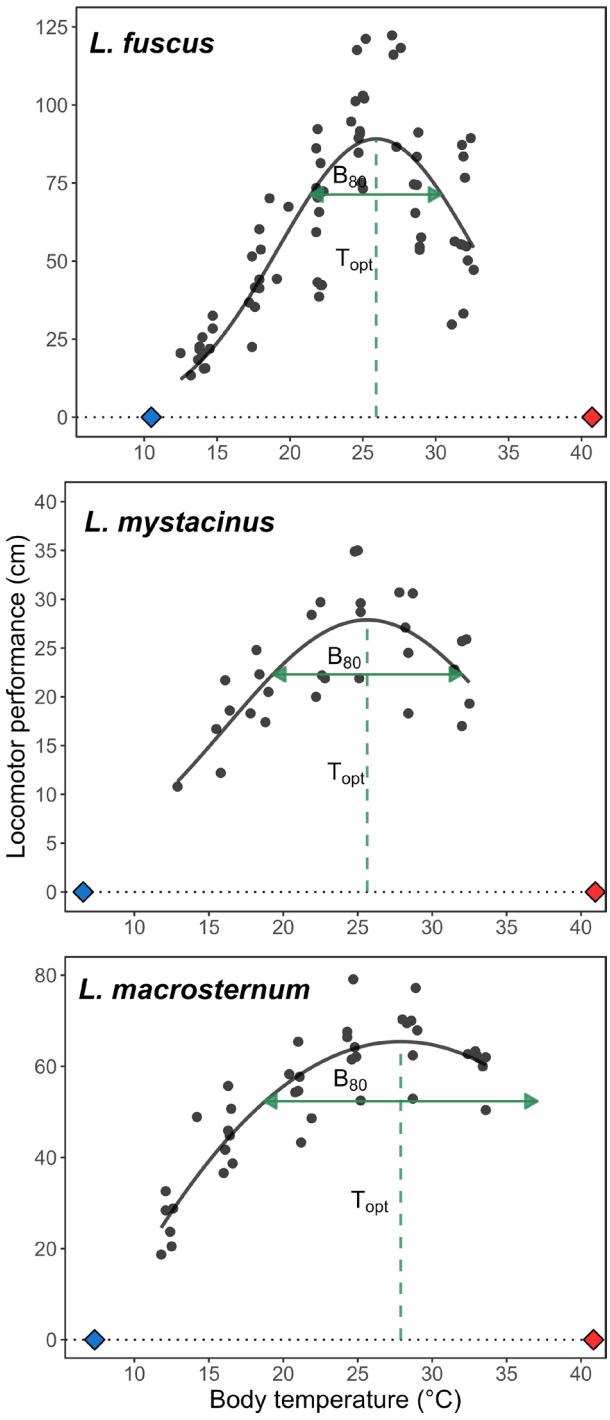



Figure 1.Empirical thermal performance curves for the longest distance (cm) jumped by *Leptodactylus fuscus*, *L. mystacinus*, and *L. macrosternum* Neotropical anurans. Green vertical dashed lines indicate the optimal temperature ($T_{opt}$), green horizontal arrows indicate the thermal range at which locomotory function remains above 80% of its maximum capacity (i.e. the $B_{80}$), and head arrows indicate the $B_{80}$ lower and upper limits, respectively. Diamonds indicate the empirically determined $CT_{min}$ (blue diamond) and $CT_{max}$ (red diamond). Filled circles depict individual frog's $T_b$ and the black solid line indicates the best fitted curve found for jumped observations.



16000587, 2026, 1, Downloaded from https://nsojournals.onlinelibrary.wiley.com/doi/10.1002/ecog.07617 by Universidade Estadual Paulista, Wiley Online Library on [04/09/2026]. See the Terms and Conditions (https://onlinelibrary.wiley.com/terms-and-conditions) on Wiley Online Library for rules of use; OA articles are governed by the applicable Creative Commons License

overestimate potential activity levels, as voluntary thermal limits in nature are less extreme than critical temperatures (Rezende et al. 2014).

The rates of EWL from animals were measured at different temperatures (15, 20, and 25°C) using an open flow-through system (i.e. without recirculating the system airstream). This system consisted of a continuous dry airflow (< 1% relative humidity; RH) that ventilated a chamber containing the animal while the air humidity leaving the chamber was continuously monitored using an RH analyzer connected to a computer. From these data, we calculated the absolute EWL ($gH_2O\ h^{-1}$) rates for each species (see Maenaka et al. (2023) for experimental setup details). We also determined the species' ability to tolerate dehydration by exposing previously 100% hydrated frogs to a wind tunnel until they lost the righting reflex response (Hillman 1980, Carey and Zelick 1993). At this point, frogs were weighed again, and their dehydration tolerance ($EWL_{tol}$) was calculated as the percentage (%) of body mass lost relative to their fully hydrated initial mass (see the Supporting information for a summary of physiological parameters). $EWL_{tol}$ was used as the hydric physiological threshold for the cessation of activity in our computing simulations.

The permit for the animal collection was issued by the Instituto Chico Mendes da Conservação da Biodiversidade, Brazil (JCMBIO-MMA, no. 22028). All procedures and experimental protocols were approved by the Ethics Committee for the Use of Animals in Research, CEUA-Unesp (protocol no. 2570, 6915, and 5909).

## Thermal and hydric ecological modeling

### *Species distributional areas*

We restricted our analysis to the South American region, which encompasses the known distribution of the studied species (Sá et al. 2014, Magalhães et al. 2020). We delineated the distributional areas for each species based on the α-hull method (Burgman and Fox 2003). This technique yields geographical range estimates by fitting Delauney α-hull polygons (Delauney triangulation) around species presence records (Supporting information). Presence records were obtained from the Global Biodiversity Information Facility portal (GBIF; www.gbif.org) for *L. fuscus* and *L. mystacinus*. For *L. macrosternum*, we used georeferenced records from Magalhães et al. (2020), which offer updated and revised occurrence data for this species. After a data cleaning procedure to remove suspicious records (detailed in the Supporting information), we used 2901 records for *L. fuscus*, 258 for *L. mystacinus*, and 265 for *L. macrosternum*.

Because available occurrence data constrain polygonal range delimitation, spatial coverage can suffer discontinuities due to sampling gaps in areas that may represent suitable locations for species presence (Marsh et al. 2023), especially in under-sampled regions such as the Neotropics (Fouquet et al. 2007). Therefore, we used predicted presences from species distribution models (SDM) to reduce potential geographical gaps of suitable areas and to complement our previous polygonal range delimitations (Pena et al. 2014, Syfert et al. 2014). We constructed SDMs by relating species presence records (used for polygonal range delimitations) to bioclimatic variables obtained from the WorldClim database (www.worldclim.org). We selected them for their ecological relevance and low spatial collinearity. We used an ensemble modeling technique (Araújo and New 2007), in which the outputs of multiple predictive models were combined to estimate species habitat suitability, with values ranging between 0 and 1 (see the Supporting information for full details on bioclimatic variable selection and SDM procedures). Suitability maps were then converted into binary maps (0 = unsuitable and 1 = suitable) by applying the lowest presence threshold (LPT; Pearson et al. 2007), a method that sets the lowest suitability value by which all grid cells equal to (or better than) those containing a species record are retained, thus minimizing omission error (Pearson et al. 2007). The LPT also accounts for moderately suitable yet feasible locations for the species presence that more restrictive methods would otherwise overlook (Peterson and Raghavan 2017). Finally, the LPT maps were superimposed on the polygonal range estimates to produce a derived range delimitation. Although SDM presence predictions can suffer from the same under-sampling issues as polygonal delimitations, SDMs are a relatively robust alternative to complement polygonal range estimates (Pena et al. 2014, Syfert et al. 2014). Furthermore, this combined approach yielded better spatial continuity with broader environmental conditions, which is well suited for the aims of the present study.

### Microclimatic conditions

We used the existing 'microclim' dataset of Kearney et al. (2014) to estimate species responses to ambient conditions at the organismal level. This ready-to-use microclimatic dataset was built using the 'NicheMapR' R package (Kearney and Porter 2017). It uses biophysical modeling to estimate climatic parameters at the microhabitat level, based on the input of various descriptors for 24 hours of a monthly day at a 15 km spatial resolution. We extracted microclimatic conditions at various shading levels (0, 25, 50, 75, and 90%) of wind speed, relative humidity, solar radiation, soil surface (and 5 cm below surface) temperatures, and air temperature 1 cm above the ground (Kearney et al. 2014). Our model species exhibit a wide geographical distribution (Sá et al. 2014, Magalhães et al. 2020), which covers different biomes with contrasting vegetation structures (Hansen et al. 2013). In this regard, one variable of particular relevance to our study is the differences in canopy cover. We assigned each microclimatic grid cell a representative canopy-shading level and retained only the appropriate shading microclimate features corresponding to each respective cell. These shading levels were derived from a 30-m resolution tree cover map (Hansen et al. 2013), which was upscaled to a 15-km resolution and reclassified into five canopy classes (0, 25, 50, 75, 90%) (the Supporting information contains further details).



16000587, 2026, 1, Downloaded from https://nsojournals.onlinelibrary.wiley.com/doi/10.1002/ecog.07617 by Universidade Estadual Paulista, Wiley Online Library on [04/09/2026]. See the Terms and Conditions (https://onlinelibrary.wiley.com/terms-and-conditions) on Wiley Online Library for rules of use; OA articles are governed by the applicable Creative Commons License

A second issue with our species' wide distribution is their seasonal activity period, which varies by region. For example, in their southernmost distribution, *L. fuscus* and *L. mystacinus* are primarily active between December and April (Abe and Garcia 1991, Lucas et al. 2008), while in the central region, activity occurs mainly between August and November (De-Carvalho et al. 2008). Finally, in the northern portion, *L. fuscus* is primarily active between March and July (Solano 1987, Martins 1988, Méndez-Narváez et al. 2015). Similarly, *L. macrosternum* activity begins in December in the south (Prado et al. 2000) and in May in the north (Chaves et al. 2021), aligning with regional rainy seasons (Alvarez et al. 2014). To account for this regional effect on phenology, we set cell-specific seasonal periods of activity. In our target modeling areas, the climate generally consists of a 4–6-month wet summer and a dry–cold winter (more pronounced at higher latitudes). Still, *Leptodactylus* activity largely coincides with wet months when seasonal rainfall is concentrated (Maffei et al. 2011, Haddad et al. 2013). Therefore, we identified the most humid month as the frogs' peak activity period and used it to define an asymmetric six-month activity window (two months before and three months after the peak), representing three simplified seasonal activity phases: 1) early season (emergence from aestivation as rains begin and humidity levels rise), 2) mid-season (during their peak activity, which often coincides with highest humidity due to heavier rainfalls), and 3) late season (when activity and humidity levels gradually decline as the wet season ends). We accomplished this by separating the 12-month stacked microclimate raster layers by month and identifying, for each grid cell, the wettest month (i.e. the month with the highest daily average RH). We then retained the microclimatic data for this peak month, along with data from two months prior to and the third month after the peak. The assumption of asymmetry for the six-month activity window reflects the unequal potential for frog activity, as ambient humidity is low in both the early and late seasons, but water bodies formed by accumulated rains persist longer in the latter, allowing for prolonged potential activity (Vieira et al. 2007, Maffei et al. 2011, Silva 2016).

#### *Body temperature and evaporative water loss evaluation*

To link frogs to the ground-level microclimate, we first solved the expected inflows and outflows of heat energy for $T_b$ using the biophysical model described by Rubalcaba et al. (2019b). Briefly, the model builds on heat exchange mechanisms for ectotherms, as described by Porter et al. (1973), calculating the steady-state $T_b$ by balancing heat inflows (solar and longwave radiation) and outflows (air convective heat flow, conduction to the ground, and cutaneous evaporative cooling). It should be noted that longwave radiation, convection, and conduction can act as either inflows or outflows depending on the temperature gradients between the organism and its environment. These heat exchanges are a function of both species-specific morphological features (body size and posture, which affects body surface-to-volume ratios (SA:V) and proportions of skin surface area exposed to body heat/mass fluxes, body heat capacity, and skin resistance to evaporation) and the local hourly microclimate conditions described above (see Rubalcaba et al. (2019b) for a detailed explanation). This biophysical model has already been validated by empirical observations of more than 40 lizards (Rubalcaba et al. 2019b). Here, we evaluated its predictive performance using thermal data from wet-skinned (agar models) deployed under field conditions. Agars serve as a simplified yet effective method for approximating the evaporative properties of equivalent-sized living animals and are a well-established approach for field thermal studies (Nowakowski et al. 2017, Anderson et al. 2018, Lertzman-Lepofsky et al. 2020, Ortega-Chinchilla et al. 2022). Even though agar models do not replicate the physiological processes at play in live animals, they provide an approximation of the passive water exchange between a generalized amphibian with negligible or no cutaneous resistance to water loss and the environment (Riddell et al. 2017). We used the agar model results to evaluate the biophysical model over a wide temporal window (various days), as it provides continuous operative thermal measures. We deployed agar models of various sizes (5, 23, 28, and 112 g) in the field over sunny and shady locations and monitored their core temperatures using thermal data loggers for six consecutive days. This agar deployment arrangement allowed us to evaluate the biophysical model under typical but simplified size–microclimate combinations that anurans might experience (Supporting information). Concurrently, using the biophysical modeling described above, we computationally simulated the expected hourly temperatures for equivalent-sized hypothetical agars at the same sunny and shady locations as the real agar models. To compare the congruency between these two approaches, we generated temperature curves from simulations and mean hourly field observations ($T_b$ collected from real agar models) and evaluated the similarity between them via discrete Fréchet distance (DFD) analysis (Eiter and Mannila 1994, Cui et al. 2022). This metric measures the dissimilarity between two curve shapes. The lower the value, the more similar the curves are.

Evaporative cooling is an essential component of the organismal heat budget. The biophysical model incorporates this effect by estimating the expected rate of cutaneous EWL based on key organismal attributes, environmental conditions, and physical principles governing mass transfer (the same as for heat exchange, as mentioned above). We used the empirically determined EWL rates for the three studied species to evaluate the EWL accuracy estimated by the biophysical model. For this, we first identified grid cells in our microclimate dataset that had a combined profile of wind speed ($1 \pm 0.1$ m $s^{-1}$) and air and ground temperatures (15, 20, 25°C with a $\pm$ 1°C variation) that closely matched our experimental conditions of airflow rate (21 $cm^3 s^{-1}$) and test temperatures (15, 20, 25°C) used in living frogs. For these same grid cells, we used the biophysical model to simulate the expected EWL for a theoretical 9 g *L. fuscus*, 15 g *L. mystacinus*, and 57 g *L. macrosternum* (the average mass of our measured living frogs) represented by an anuran-like ectotherm with species-specific morphological characteristics



16000587, 2026, 1, Downloaded from https://nsojournals.onlinelibrary.wiley.com/doi/10.1002/ecog.07617 by Universidade Estadual Paulista, Wiley Online Library on [04/09/2026]. See the Terms and Conditions (https://onlinelibrary.wiley.com/terms-and-conditions) on Wiley Online Library for rules of use; OA articles are governed by the applicable Creative Commons License

(see the Supporting information for model settings). We then compared the evaporative water loss between these two approaches at different temperatures using generalized linear mixed-effect models (GLMM). We run this analysis separately for each species, with the interaction between source (simulations versus empirical measures) and temperature (15, 20, and 25°C) as fixed factors, the identity of living frogs as a random factor, and EWL as the response variable. GLMMs were followed by Tukey's tests to identify significant differences at each temperature.

The empirically derived and biophysically calculated $T_b$ and EWL were compared using DFD and GLMM analyses, respectively, as overall congruency measures, whereas hourly temperature deviations were used as diagnoses for hourly $T_b$ congruency. While not identical, the level of congruency between empirical and biophysical $T_b$ estimations (particularly in shady conditions) deviated, on average, equal to or less than 2.7°C (Supporting information). Similarly, although the EWL differed at some species-specific test temperatures (varying between 6.2 and 28.5%; Supporting information), the empirical and biophysical calculations coincided with others (see Results). Based on these results, we accepted the level of congruency for the empirical versus biophysical estimations (Supporting information) and proceeded with biophysical projections in all further analyses.

### Activity and environmental restrictions

We simulated the hourly $T_b$ distribution for a theoretical 9 g *L. fuscus*, 15 g *L. mystacinus*, and 57 g *L. macrosternum* at 1 cm above ground conditions. As nocturnal frogs, we allowed surface activity across all nighttime hours (18:00–05:00 h) and assumed that animals retreat to underground refugia (become inactive) during the daylight hours (06:00–17:00 h) (Silva and Giaretta 2008, Henrique and Grant 2019). Because simulations incorporate a body thermal inertia (i.e. the $T_b$ at a given hour is influenced by the $T_b$ in the previous time step hour), we assumed that animals start activity (18:00 h) with a $T_b$ matching their retreat site temperature the hour before emergence (17:00 h). Our simulations focused primarily on organismal-based heat and water exchange processes to infer environmental constraints. We implemented two interactive subroutines that simulated simple behavioral responses based on the organism's internal temperature state (thermal sensitivity of locomotor performance) and hydration (dehydration thresholds derived from cumulative EWL).

First, we used the thermal sensitivity of locomotor performance from empirical TPC to infer habitat thermal suitability. We set $CT_{min}$ and $CT_{max}$ as the lower and upper thermal thresholds at which activity ceases due to locomotor impairment (i.e. the 'thermal activity timeframe' in our simulations). Within this thermal timeframe, we adopted a temperature-dependent probability of activity following Gunderson and Leal (2016), in which the surface activity transitions from zero (defined by physiological limits) to greater than zero (dictated by organismal performance capabilities). This smooth transitional model of activity patterns has proven to be very effective in predicting empirical observations of lizard species (Rozen-Rechels et al. 2020). Therefore, our models assume that frogs with a $T_b$ within their thermal performance breadth ($B_{80}$) are physiologically capable of conducting most ecological tasks and, as a result, are always active at the surface (100% probability of activity) unless severely dehydrated. Beyond these limits, performance, and hence the probability of activity, rapidly decreases following the descending portions of locomotor TPC until performance reaches zero (i.e. as set by the lower and upper thermal thresholds). To account for the potential costs associated with hydric stress, we incorporated the sensitivity to EWL (derived from the EWL simulated by the biophysical model) as a potential constraint for activity. We assumed that the animals were fully hydrated at the time of shelter emergence. From this point on, we computed the hourly cumulative EWL ($gH_2O\ h^{-1}$) until it reached the maximum body water loss tolerance ($EWL_{tol}$) by *L. fuscus* (38.49%), *L. mystacinus* (35.53%), and *L. macrosternum* (31.78%). The 'hydric activity timeframe' was defined as the time (total hours) between emergence and reaching the dehydration threshold (the $EWL_{tol}$), assuming no further activity or rehydration during this period. Regardless of the hydration level, this hydric activity timeframe can be curtailed at any time if the animal attains a critical thermal threshold. In summary, we considered that frogs would retreat to underground shelter during nighttime hours if they experienced harmful temperatures ($CT_{min}$ or $CT_{max}$) or chronic hydric deficits ($EWL_{tol}$) and during all the daytime hours.

Although frogs are nocturnally active, daytime shelters can also affect their thermal budgets (Forget-Klein and Green 2021). In nature, our species tend to build burrows in very wet soils (Solano 1987, Silva and Giaretta 2008) at depths of approximately 5–9 cm, depending on the species (Martins 1988, Lucas et al. 2008, Oliveira-Filho and Giaretta 2008). Based on their burrow characteristics, we assumed frogs to be 5 cm deep and fully hydrated when sheltered. We used the hourly substrate temperature 5 cm below the surface as a proxy measure for sheltering $T_b$ because sheltered animals will inevitably attain thermal equilibrium with their shelters shortly (Smits 1984). Note that 'sheltering' is a facultative state during activity that permits animals to escape harmful surface conditions. However, during daytime, sheltered frogs will perish if their $T_b$ are not between $CT_{min}$ and $CT_{max}$, thus rendering those geographical locations (grid cells) unsuitable to be occupied.

### Suitability maps

To identify the physiologically limiting constraints on activity across the entire geographical distribution of the species, we identified for grid cells in which the activity time was curtailed before nighttime hours were completed, the hours of restrictions (Hr: nighttime hours of inactivity due to thermal and hydric constraints), and the respective traits responsible for this cessation ($CT_{min}$, $CT_{max}$, or $EWL_{tol}$). The resulting grid cell output was then spatially rasterized into new raster layers to represent the potential physiological constraints on activity in a geographic space. Based on these spatial physiological



16000587, 2026, 1, Downloaded from https://nsojournals.onlinelibrary.wiley.com/doi/10.1002/ecog.07617 by Universidade Estadual Paulista, Wiley Online Library on [04/09/2026]. See the Terms and Conditions (https://onlinelibrary.wiley.com/terms-and-conditions) on Wiley Online Library for rules of use; OA articles are governed by the applicable Creative Commons License

outputs, we also calculated the percentage of these Hr grid cells relative to the total geographical distribution of the species.

The production of suitability maps involved two steps. First, a thermal and hydric suitability map was produced separately by considering the two primary physiological criteria (thermal performance and body hydration thresholds) used to infer environmental constraints in our simulations. Then, the resulting suitability maps were overlaid to produce a derived map representing the joint suitability as a function of the thermal and hydric criteria. From a thermal standpoint, our models were constructed based on thermal thresholds bounding temperature-dependent activity probabilities (dictated by organismal performance capabilities), all related to the hourly microclimate. Hence, for a continuously active frog, the thermal thresholds and probabilities of activity will vary hourly as the nightly thermal conditions change over time. For this reason, we quantified a location's thermal suitability by scaling hourly surface activity scores between 0 (least suitable) if the animal was impeded from engaging in activity due to thermal restrictions (0 h of activity) and 1 (highly suitable) if the animal achieved at least 6 h of activity with its $T_b$ kept within the $B_{80}$ limits. This assumption is based on field observations of some leptodactylid species, whose activity occurs primarily during the first half of the night (Woolbright 1985, De-Carvalho et al. 2008, Bardier et al. 2014).

On the other hand, unlike thermal traits, EWL is a cumulative process that occurs hourly (sum across hours) until it attains the physiological endpoint defined by $EWL_{tol}$. Hence, the hydric suitability of locations was estimated by scaling the total cumulative EWL scores into relative scores ranging from 0 (least suitable) when the cumulative EWL reached $EWL_{tol}$ during the first hour of activity (0 h of activity due to hydric restrictions) to 1 (highly suitable) if the animal was able to be active at night with a cumulative EWL less than 1% of its initial state of complete hydration. Finally, we combined the thermal and hydric suitability maps by averaging their scores to produce a joint suitability map ranging from 0, where either thermal or hydric restrictions curtailed activity, and 1, where animals could maintain an optimal range of $T_b$ (at least 6 h of activity within their $B_{80}$ limits) and a good hydration level.

## Results

In general, the overall agreement of hourly predictions and observations was better in shady (DFD = 1.48 for 28 g agars; DFD = 1.56 for 5 g agars) than in sunny locations (DFD = 5.36 for 112 g agars; DFD = 5.83 for 23 g agars). There was an average hourly SD of 1.28°C for 28 g agars (maximum SD of 3.09°C), 1.32°C for 5 g agars (maximum SD of 3.16°C), 2.67°C for 112 g agars (maximum SD of 6.96°C), and 2.56°C for 23 g agars (maximum SD of 7.42°C). Simulated and empirical EWL differed for *L. fuscus* ($\chi^2_2 = 57.06$, $p < 0.001$), *L. mystacinus* ($\chi^2_2 = 41.27$, $p < 0.001$), and *L. macrosternum* ($\chi^2_2 = 41.98$, $p < 0.001$), this difference being significant ($p < 0.05$) at 20°C for *L. fuscus*, at 15 and 25°C for *L. mystacinus*, and 15 and 20°C for *L. macrosternum* (Supporting information).

Considering only the period in which frogs were active, $CT_{min}$ imposed a variable number of hours of restriction (Hr) on all species within their current geographic distribution across early, mid, and late seasons. $EWL_{tol}$ also imposed restrictions, but only on the smallest species, *L. fuscus*. On average, considering only the grid cells where the animals experienced some restriction, *L. fuscus* was restricted by a nightly Hr of 3.5, 3.2, and 3.6 h for the early, mid, and late seasons, respectively. These restrictions covered 36.5, 10.2, and 41.0% of the total distribution of *L. fuscus* for the early, mid, and late season, respectively. The mid-sized species, *L. mystacinus*, was restricted by a nightly average of 2.7, 6.1 and 6.7 Hr for the early, mid, and late seasons, with activity constraints covering 8.7, 14.3, and 21.9%, respectively, of its total distribution. The large species, *L. macrosternum*, experienced the least nightly restriction overall, averaging 1.5, 4.1, and 4.1 Hr for the early, mid, and late season, and covering 3.4, 6.0, and 7.3% of its distribution, respectively. However, the responsible constraint for activity was not geographically uniform among species. In *L. fuscus,* restrictions occurred mainly along the southern border of its distribution due to $CT_{min}$ (Fig. 2A–C) and in the central and eastern regions due to $EWL_{tol}$, particularly during the early and late season (Fig. 2D–F). In *L. mystacinus* and *L. macrosternum*, restrictions occurred mainly at the southern limits of their distributions due solely to $CT_{min}$, and it was particularly evident during the mid and late season (Fig. 2G–I, J–L, respectively). No species attained $CT_{max}$ during activity across their entire distribution.

Suitability maps revealed that central and northern regions provide suitable thermal conditions for all three species, where animals can maintain at least 6 h of activity within an optimal range of $T_b$ (i.e. within their $B_{80}$ limits), particularly during the mid-season (Fig. 3A–D, 4A–D, and 5A–D). On the other hand, hydric conditions were more suitable (i.e. areas with lower cumulative EWL during activity) in the southern limits of *L. fuscus* (Fig. 3E–G), the southern portion of the distribution of *L. mystacinus* (Fig. 4E–G), and almost the entire distribution of *L. macrosternum* (Fig. 5E–G). Moreover, for *L. fuscus*, hydric suitability was lower during the early and late season (Fig. 3H), and more generally, its overall hydric suitability was much lower than that of the other two larger species, whose hydric suitability tended to remain consistent across seasonal phases (Fig. 4H, 5H, respectively). The combination of the thermal and hydric suitability maps clearly showed that the level of suitability varied spatially based on species-specific temperature locomotor sensitivity and hydric requirements (Fig. 3I–L, 4I–L, 5I–L).

## Discussion

Our results pointed out that the level of time restriction in activity varied among the three *Leptodactylus* species across



16000587, 2026, 1, Downloaded from https://nsojournals.onlinelibrary.wiley.com/doi/10.1002/ecog.07617 by Universidade Estadual Paulista, Wiley Online Library on [04/09/2026]. See the Terms and Conditions (https://onlinelibrary.wiley.com/terms-and-conditions) on Wiley Online Library for rules of use; OA articles are governed by the applicable Creative Commons License

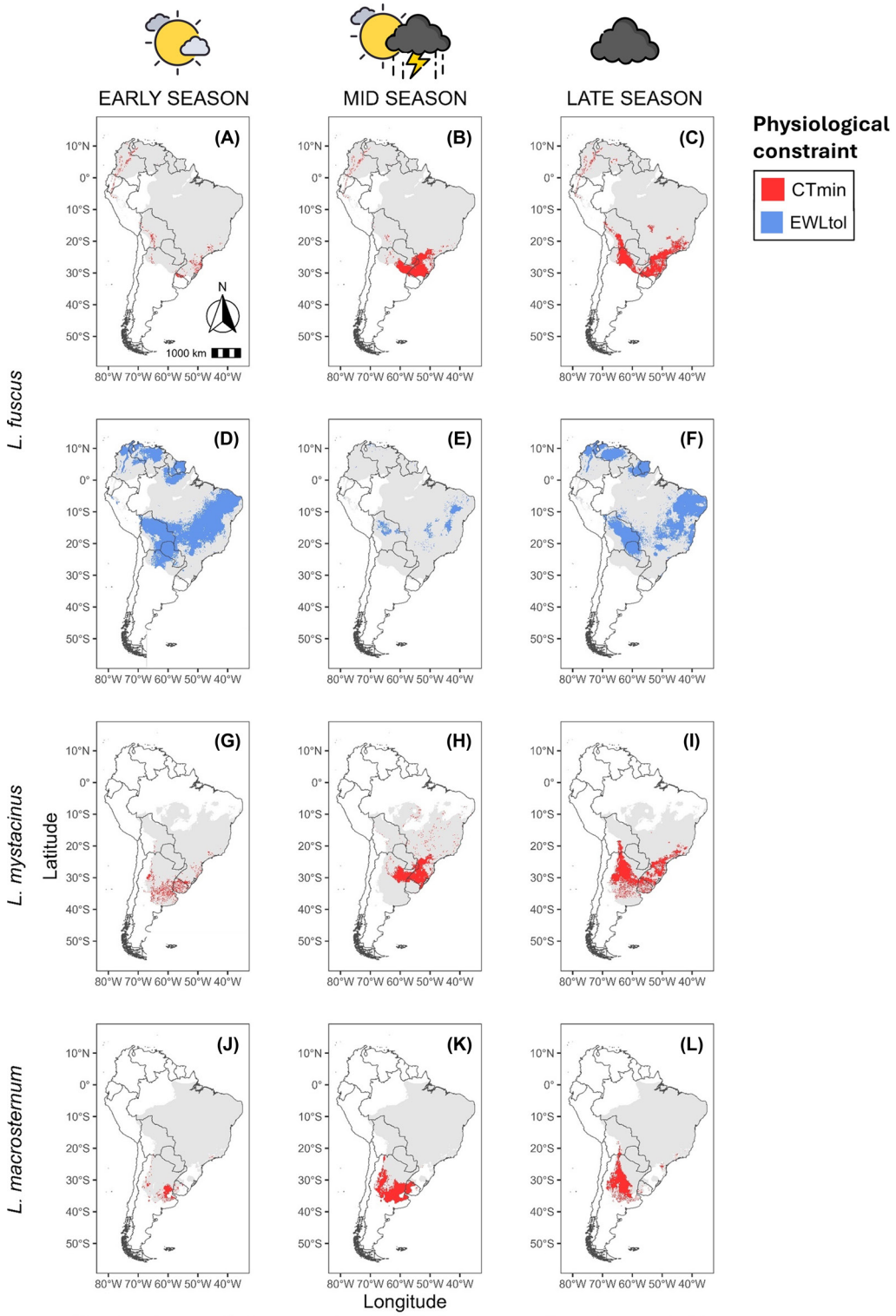



Figure 2. Spatial physiological constraints on activity time derived from mechanistic simulations for *Leptodactylus fuscus* (A–F), *L. mystacinus* (G–I), and *L. macrosternum* (J–L). The top section shows the frogs' seasonal activity phases: when they emerge with the first seasonal rains (early season), during their period of maximal activity in the most humid month (mid-season), and when their activity gradually reduces as the rainy season ends (late season). Gray areas indicate the species' distribution ranges. Areas in red are locations where the animals reached their critical thermal minimum ($CT_{min}$), and areas in blue where they reached their dehydration tolerance ($EWL_{tol}$) during activity, regardless of the total hours of restrictions. Consequently, these areas also represent locations where species presence is mediated by the buffering effect of shelter use. $EWL_{tol}$ areas are absent for *L. mystacinus* and *L. macrosternum*, as these species never reached their $EWL_{tol}$ threshold during activity.



16000587, 2026, 1, Downloaded from https://nsojournals.onlinelibrary.wiley.com/doi/10.1002/ecog.07617 by Universidade Estadual Paulista, Wiley Online Library on [04/09/2026]. See the Terms and Conditions (https://onlinelibrary.wiley.com/terms-and-conditions) on Wiley Online Library for rules of use; OA articles are governed by the applicable Creative Commons License

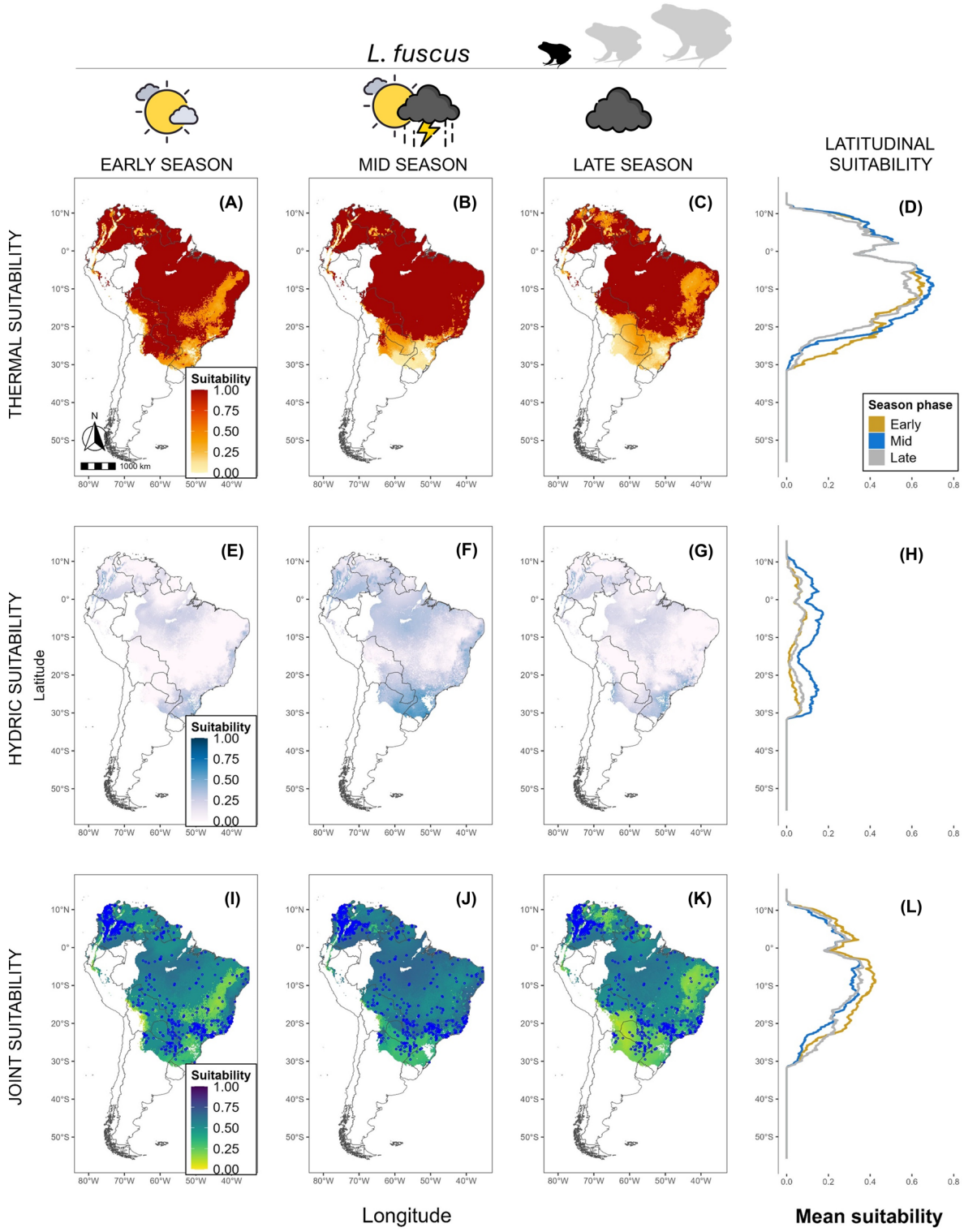



Figure 3. Spatially explicit thermal suitability (A–C), hydric suitability (E–G), and joint suitability (a combination of hydric and thermal suitability; I–K) for the Neotropical frog *Leptodactylus fuscus*. Latitudinal suitability represents the mean suitability across the species' latitudinal range during the early (orange line), mid (blue line), and late (gray line) frog activity season for thermal (D), hydric (H), and joint suitability (L) maps. The darker frog silhouette at the top indicates the body size of *L. fuscus* (small) relative to the other two studied species. Blue points on the joint suitability maps represent known presence records for the species (see the Supporting information for details on presence records).



16000587, 2026, 1, Downloaded from https://nsojournals.onlinelibrary.wiley.com/doi/10.1002/ecog.07617 by Universidade Estadual Paulista, Wiley Online Library on [04/09/2026]. See the Terms and Conditions (https://onlinelibrary.wiley.com/terms-and-conditions) on Wiley Online Library for rules of use; OA articles are governed by the applicable Creative Commons License

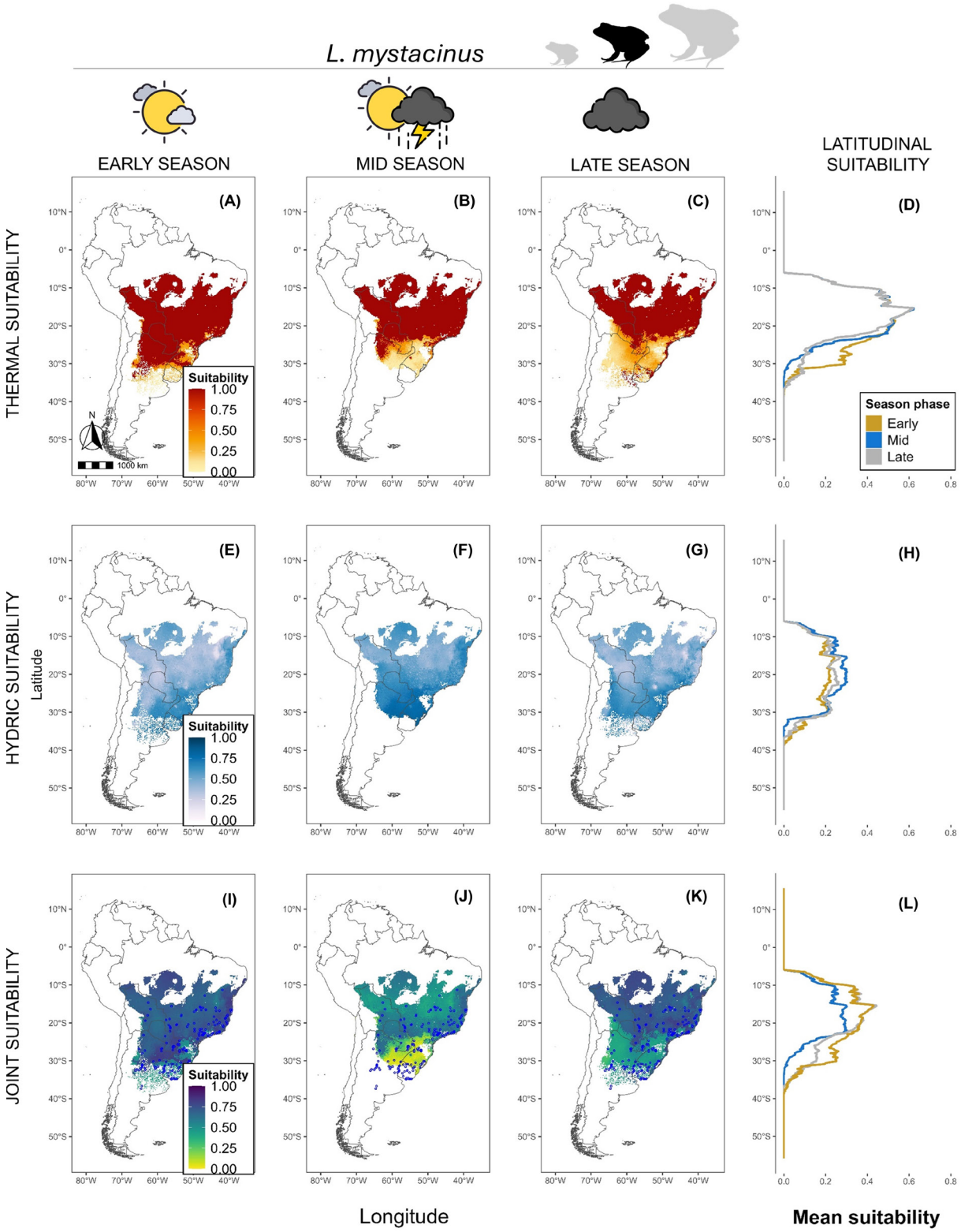



Figure 4. Spatially explicit thermal suitability (A–C), hydric suitability (E–G), and joint suitability (a combination of hydric and thermal suitability; I–K) for the Neotropical frog *Leptodactylus mystacinus*. Latitudinal suitability represents the mean suitability across the species' latitudinal range during the early (orange line), mid (blue line), and late (gray line) frog activity season for thermal (D), hydric (H), and joint suitability (L) maps. The darker frog silhouette at the top indicates the body size of *L. mystacinus* (medium) relative to the other two studied species. Blue points on the joint suitability maps represent known presence records for the species (see the Supporting information for details on presence records).



16000587, 2026, 1, Downloaded from https://nsojournals.onlinelibrary.wiley.com/doi/10.1002/ecog.07617 by Universidade Estadual Paulista, Wiley Online Library on [04/09/2026]. See the Terms and Conditions (https://onlinelibrary.wiley.com/terms-and-conditions) on Wiley Online Library for rules of use; OA articles are governed by the applicable Creative Commons License

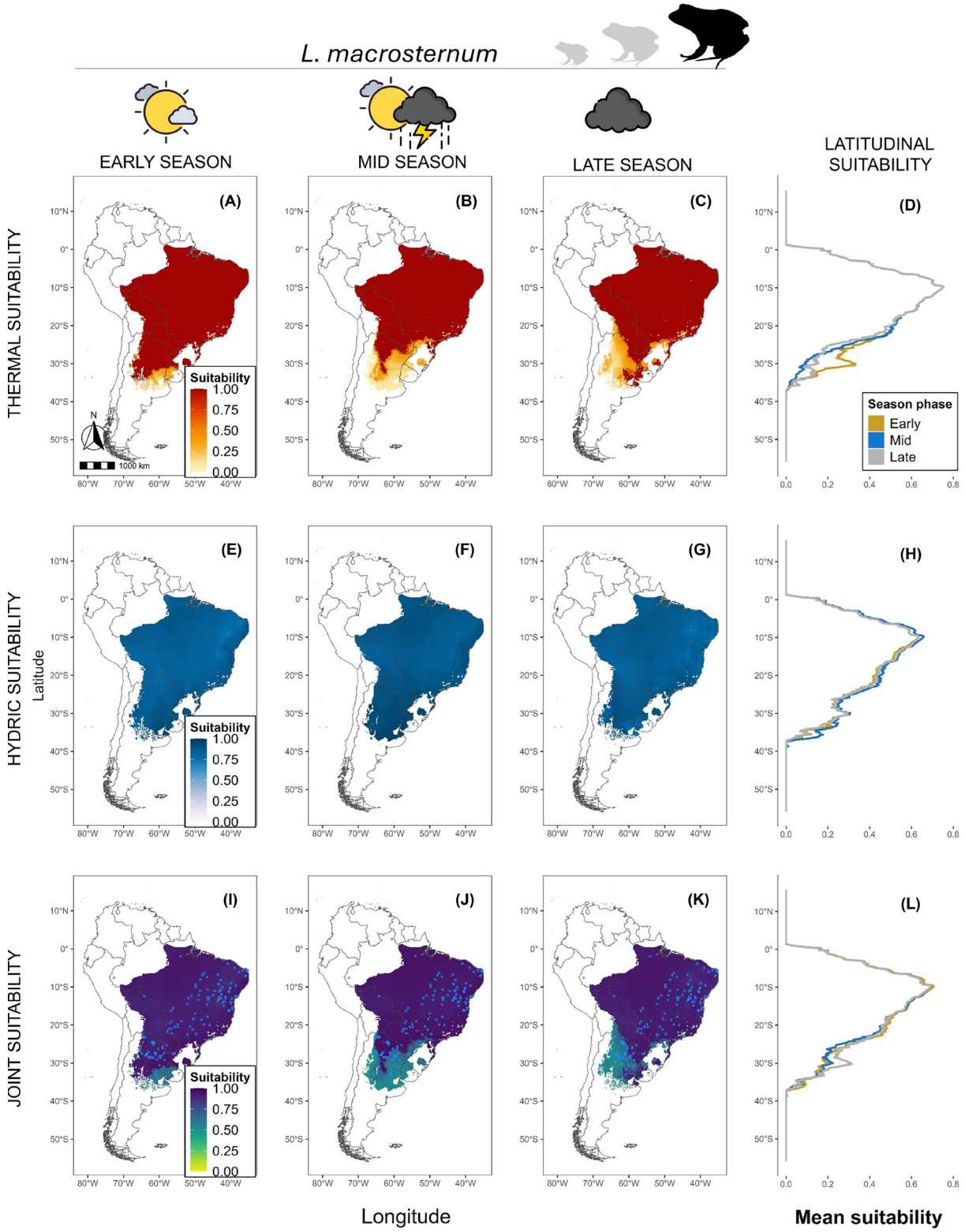



Figure 5. Spatially explicit thermal suitability (A–C), hydric suitability (E–G), and joint suitability (a combination of hydric and thermal suitability; I–K) for the Neotropical frog *Leptodactylus macrosternum*. Latitudinal suitability represents the mean suitability across the species' latitudinal range during the early (orange line), mid (blue line), and late (gray line) frog activity season for thermal (D), hydric (H), and joint suitability (L) maps. The darker frog silhouette at the top indicates the body size of *L. macrosternum* (large) relative to the other two studied species. Blue points on the joint suitability maps represent known presence records for the species (see the Supporting information for details on presence records).



16000587, 2026, 1, Downloaded from https://nsojournals.onlinelibrary.wiley.com/doi/10.1002/ecog.07617 by Universidade Estadual Paulista, Wiley Online Library on [04/09/2026]. See the Terms and Conditions (https://onlinelibrary.wiley.com/terms-and-conditions) on Wiley Online Library for rules of use; OA articles are governed by the applicable Creative Commons License

seasonal phases, reflecting their different sensitivity to thermal and hydric conditions. During the early, mid, and late seasons, *L. mystacinus* had the highest restriction on activity time (averaging 2.7, 6.1, and 6.7 Hr, respectively), followed by *L. fuscus* (3.5, 3.2, and 3.6 Hr), and *L. macrosternum* (1.5, 4.1, and 4.1 Hr). Despite showing more consistent restriction levels across seasonal phases, the smallest species, *L. fuscus*, faced greater constraints in the early and late phases, mostly due to its high rates of EWL rather than thermal constraints. Conversely, the large size of *L. macrosternum* conferred a greater capacity to retain body water, resulting in low and consistent seasonal water constraints, yet more variable thermal restrictions, particularly in the mid and late phases. Still, it exhibited the lowest overall activity restrictions across all periods compared to the other two species. *Leptodactylus mystacinus*, with its more southerly distribution (compared to the other two species), disproportionately faced the most significant thermal restrictions due to the colder conditions at higher latitudes, especially during the late season when cooler temperatures predominate.

Restriction in activity was linked to $CT_{min}$ for all three species and $EWL_{tol}$ for *L. fuscus*. This finding contrasts with most assessments linking activity restriction in ectotherms to increasing temperatures, particularly true for squamate reptiles (Sinervo et al. 2010, Kearney 2013, Sears et al. 2016, Kearney et al. 2018), but also in some anuran species (Enriquez–Urzelai et al. 2019, Lertzman-Lepofsky et al. 2020). Indeed, the prevalent view is that tropical ectotherms operate at temperatures closer to their upper thermal tolerance and are more likely to be constrained by warmer temperatures. We argue that this view may be restricted to diurnal thermoregulator squamates, which have dominated studies on this theme. Our results, however, show that this is not a general rule, particularly in the case of nocturnally active anurans, with similar evidence in some other anuran species and salamanders (Beukema et al. 2021). None of the three *Leptodactylus* species we studied reached their upper thermal threshold for activity ($CT_{max}$). In fact, their $T_b$ distribution during activity was below their optimal performance temperature and upper thermal $B_{80}$ limit (Supporting information). Thus, the only thermal restriction identified was caused by lower temperatures, especially during the late season and along the southern border of their distribution, characterized by colder habitats. Our findings do not oppose previous claims about the susceptibility of tropical species to climate change (Deutsch et al. 2008, Duarte et al. 2012, Scheffers et al. 2013, Simon et al. 2015). Instead, they highlight the pervasiveness of the lower thermal bound for activity and suggest that overemphasizing upper thermal limits may provide an incomplete understanding of climatic constraints on anurans, particularly those with nocturnal behavior.

Our models assume continuous activity during the entire nighttime, and this assumption may have influenced some of the restriction outcomes just discussed. For example, most *Leptodactylus* frogs are more active during the first half of the night (Woolbright 1985, De-Carvalho et al. 2008, Bardier et al. 2014) coinciding with the warmest nighttime hours (Zina and Haddad 2005, Chaves et al. 2017, Henrique and Grant 2019). However, most of the predicted restrictions on activity associated with low temperature were identified by our simulations at the end of the night (Supporting information). Thus, the impact of this particular restriction may not be as strong as estimated. Also, the pattern of nightly activity is likely to change across the different phases of the activity season and among the species. Unfortunately, a detailed behavioural assessment of the patterns of activity in *Leptodactylus* is not available, precluding us from refining the temporal resolution of our models to account for such potential effects.

Suitable regions have average conditions generally below the species' $T_{opt}$, and these lower temperatures also account for lower EWL rates, which might explain, at least partially, why the studied *Leptodactylus* frogs were less constrained by water in our models. The unfavorable surface-to-volume ratio of smaller species also leads to faster dehydration, which results in interspecific differences in the magnitude of such water constraints. The hydric-restricted regions for the smaller species, *L. fuscus* and *L. mystacinus*, reflected this effect, even though these areas were thermally suitable for performance. We found these conditions to occur mainly in Brazil's central and northernmost regions, where drier conditions markedly reduced hydric suitability for *L. mystacinus* (Fig. 4E–G) and caused *L. fuscus* to lose body water to near lethal dehydration levels (Fig. 2D–F). Thermal conditions were generally most favorable during the early and mid-seasons, aligning with warmer months. In contrast, the late season exhibited reduced thermal suitability, primarily reflecting the transition from the hot–wet to the cold–dry season. The joint suitability of the small *L. fuscus* was primarily limited by its high hydric sensitivity, with thermal constraints becoming prominent in the early and late seasons. For the mid-sized *L. mystacinus*, thermal restrictions dominated its overall suitability due to its southerly distribution, with hydric restrictions playing a secondary but non-negligible role. In contrast, the large-sized *L. macrosternum* exhibits high joint suitability, facing minimal hydric restrictions and only slight thermal constraints during the late season. As a whole, mid-season peaks in rainfall and warmth create near-optimal conditions for all species, maximizing activity with lower hydric constraints, while the drier conditions of the early and late seasons, combined with colder temperatures in the latter, contribute to further restrictions for smaller species, especially at higher latitudes.

The hydric constraints identified in our study can be considered conservative, as the estimates were based on the maximum body water loss tolerance, which, although quite relevant from a functional perspective, might well surpass the voluntary tolerance limits for free-ranging frogs. Both maximum and voluntary dehydration are physiologically driven but represent different ends of the response spectrum to dehydration stress. Under mechanistic assessments, the first might better reflect a resilience threshold for activity under extreme events (e.g. drier seasonal activity months and prolonged droughts). At the same time, the latter represents plastic behavioral strategies for avoiding dehydration under routine



16000587, 2026, 1, Downloaded from https://nsojournals.onlinelibrary.wiley.com/doi/10.1002/ecog.07617 by Universidade Estadual Paulista, Wiley Online Library on [04/09/2026]. See the Terms and Conditions (https://onlinelibrary.wiley.com/terms-and-conditions) on Wiley Online Library for rules of use; OA articles are governed by the applicable Creative Commons License

conditions. Unfortunately, voluntary thresholds for dehydration remain undetermined for these and other Neotropical anurans, indicating the need for future studies to determine and incorporate them to refine hydric suitability estimates. Our results also emphasize the need to consider desiccation risks alongside upper thermal limits in diurnal ectotherms, as the interaction of higher temperatures and low humidity during peak daytime hours may further exacerbate bodily water losses, a potential limiting factor for diurnal activity (Kearney et al. 2018, Huang et al. 2020). This consideration extends to nocturnal ectotherms as well. For example, assessing activity restrictions under climate warming based solely on temperature may initially benefit nocturnal species like *Leptodactylus* frogs by reducing $CT_{min}$ constraints. However, the hydric sensitivity evaluated here suggests they could eventually face greater hydric challenges as warming intensifies, especially for smaller individuals.

Our results on thermal and hydric constraints indicate locations where frogs were forced to abandon surface activity due to heat or water stress, especially true in the drier central and colder southern regions (Fig. 2). Thus, they reflect locations where the buffering effect of shelter is particularly relevant in avoiding hydric and thermal extremes during activity. This conclusion aligns with the growing view of shelter as a key environmental component when assessing amphibian responses to climate alterations (Sunday et al. 2014, Burrow et al. 2023). The buffering potential of shelter is still dependent on the diel cycle of temperature, though, as sheltered frogs reached their $CT_{max}$ during the daytime in a few warmer coastal areas (Supporting information). One simplifying aspect of our modeling approach was adopting a dichotomous behavioral response of either being surface active or seeking underground shelter during the frogs' active period. However, this ignores possible shelter-related responses during their resting hours. Shelters represent exploitable water and thermal refugia that animals can utilize. For example, they can facilitate occasional rehydration during activity (Rittenhouse et al. 2008) or offer thermoregulatory opportunities while resting (Oromí et al. 2010, Forget-Klein and Green 2021). Depending on the context, the former would maximize activity time and the latter would aid in heat stress avoidance during the warmest part of the day. Whether resting Leptodactylid frogs actively manage their $T_b$ through the thermal properties of their burrowing system remains to be determined (Simioni et al. 2014), but adopting such an approach in species that do so certainly provides an opportunity for further improvement in estimating the overall costs of activity.

In summary, incorporating the thermal sensitivity of locomotor performance, dehydration tolerance, and the behavioral possibility of shelter use into a mechanistic assessment provided novel insights into how the activity of Neotropical anurans may be constrained by temperature and water across their geographic range. Contrary to the prevalent view of Neotropical ectotherms, we found that thermal restrictions on activity were linked to low temperatures rather than excessively warm conditions. We also identified areas where hydric conditions restrained activity, yet this effect was minor and mediated by body size, with smaller species being more vulnerable than larger ones. Moreover, the larger activity restrictions in early and late season due to the seasonal modulation of thermal and hydric constraints, especially at higher latitudes, underscore the importance of considering potential regional effects on phenology when assessing ectotherms' responses to climate variability. Our results highlight that restrictions in activity time may stem from constraints determined by different functional attributes, and that such constraints may vary among different species and along their geographic distribution.

*Acknowledgements* – We are grateful to Mariana N. Routh and Georgia K. Kosmala for their assistance with physiological data collection, and José E. Carvalho, Luisa M. Diele-Viegas, Laura Tourinho and Celio F. B. Haddad for their comments on an earlier version of the manuscript. We also thank Celso and Jacira Gavira for their hospitality at the collecting site. The São Paulo State University (UNESP) and the Center for Research on Biodiversity Dynamics and Climate Change facilitated the access to computer facilities for data processing.

*Funding* – This study was supported by the Coordination for the Improvement of Higher Education Personnel – CAPES (process no. 88882.434128/2019-01 to LMS); The São Paulo Research Foundation – FAPESP (processes no. 2007/05080-1, 2010/05473-6, 2017/17615-9, 2021/10910-0 to DVA; and 2013/50421-2, 2020/01779-5, 2021/06668-0, 2021/08322-3, 2021/08534-0, 2021/10195-0, 2021/10639-5, 2022/10760-1 to MCR); the National Council for Scientific and Technological Development – CNPq (processes no. 306811/2015-4, 302227/2019-9, 309534/2023-2 to DVA; and 442147/2020-1, 402765/2021-4, 313016/2021-6, 440145/2022-8, 420094/2023-7 to MCR; and no. 302552/2022-7, 405967/2023-3 to SFG); and the Fundação de Apoio à Pesquisa e à Inovação Tecnológica do Estado de Sergipe – FAPITEC/SE (process no. 432/2023) to SFG.

*Conflict of interest* – The authors declare no conflict of interest.

*Permits* – The permit for animal collection described in this work was issued by the Instituto Chico Mendes da Conservação da Biodiversidade, Brazil (JCMBIO-MMA, no. 22028). All procedures and experimental protocols were approved by the Ethics Committee for the Use of Animals in Research, CEUA-UNESP (protocol no. 2570, 6915 and 5909).

## Author contributions

**Luis M. Senzano**: Conceptualization (equal); Data curation (equal); Formal analysis (equal); Investigation (equal); Methodology (equal); Validation (equal); Visualization (equal); Writing – original draft (equal); Writing – review and editing (equal). **Milton C. Ribeiro**: Methodology (equal); Resources (equal); Software (equal); Supervision (equal); Validation (equal); Visualization (equal); Writing – review and editing (equal). **Sidney F. Gouveia**: Formal analysis (equal); Methodology (equal); Resources (equal); Supervision (equal); Validation (equal); Visualization (equal); Writing – review and editing (equal). **Denis V. Andrade**: Conceptualization (equal); Formal analysis (equal); Funding acquisition (equal); Investigation (equal); Methodology



16000587, 2026, 1, Downloaded from https://nsojournals.onlinelibrary.wiley.com/doi/10.1002/ecog.07617 by Universidade Estadual Paulista, Wiley Online Library on [04/09/2026]. See the Terms and Conditions (https://onlinelibrary.wiley.com/terms-and-conditions) on Wiley Online Library for rules of use; OA articles are governed by the applicable Creative Commons License

(equal); Writing – original draft (equal); Writing – review and editing (equal).

### Data availability statement

Data are available from the Dryad Digital Repository: https://doi.org/10.5061/dryad.02v6wwqhg (Senzano et al. 2025).

### Supporting information

The Supporting information associated with this article is available with the online version.

## References


Abe, A. S. and Garcia, L. S. 1991. Response to temperature in the oxygen uptake of awake and dormant frogs (Amphibia, Leptodactylidae). – Stud. Neotrop. Fauna Environ. 26: 135–141.

Alvarez, C. A., Stape, J. L., Sentelhas, P. C., Gonçalves, J. L. M. and Sparovek, G. 2014. Köeppen's climate classification map for Brazil. – Meteorol. Z. 22: 711–728.

Anderson, R. C. O., Bovo, R. P. and Andrade, D. V. 2018. Seasonal variation in the thermal biology of a terrestrial toad, *Rhinella icterica* (Bufonidae), from the Brazilian Atlantic Forest. – J. Therm. Biol. 74: 77–83.

Anderson, S. R. and Wiens, J. J. 2017. Out of the dark: 350 million years of conservatism and evolution in diel activity patterns in vertebrates. – Evolution 71: 1944–1959.

Araújo, M. B. and New, M. 2007. Ensemble forecasting of species distributions. – Trends Ecol. Evol. 22: 42–47.

Bardier, C., Canavero, A. and Maneyro, R. 2014. Temporal and spatial activity patterns of three species in the *Leptodactylus fuscus* group (Amphibia, Leptodactylidae). – S. Am. J. Herpetol. 9: 106–113.

Bestion, E., Teyssier, A., Richard, M., Clobert, J. and Cote, J. 2015. Live fast, die young: experimental evidence of population extinction risk due to climate change. – PLoS Biol. 13: e1002281.

Beukema, W., Pasmans, F., Praet, S. V., Ferri-Yáñez, F., Kelly, M., Laking, A. E., Erens, J., Speybroeck, J., Verheyen, K., Lens, L. and Martel, A. 2021. Microclimate limits thermal behaviour favourable to disease control in a nocturnal amphibian. – Ecol. Lett. 24: 27–37.

Burgman, M. A. and Fox, J. C. 2003. Bias in species range estimates from minimum convex polygons: implications for conservation and options for improved planning. – Anim. Conserv. 6: 19–28.

Burrow, A. K., McEntire, K. D. and Maerz, J. C. 2023. Estimating the potential drivers of dispersal outcomes for juvenile gopher frogs (*Rana capito*) using agent-based models. – Front. Ecol. Evol. 11: 1026541.

Carey, M. B. and Zelick, R. 1993. The effect of sound level, temperature and dehydration on the brainstem auditory evoked potential in anuran amphibians. – Hear. Res. 70: 216–228.

Cassemiro, F. S. A., Gouveia, S. F. and Diniz-Filho, J. A. F. 2012. Distribuição de *Rhinella granulosa*: integrando envelopes bioclimáticos e respostas ecofisiológicas. – Rev. Biol. 8: 38–44.

Chaves, M. F., Moura, G. J. B., Tenório, F. C. M. A., Baptista, J. S., Neto, C. J. C. L., Texeira, V. W. T. and Texeira, A. A. C. 2017. Influence of rainfall and temperature on the spermatogenesis of *Leptodactylus macrosternum* (Anura: Leptodactylidae). – Zoologia 34: 1–7.

Chaves, M. F., Moura, G. J. B., Baptista, J. S., Dantas, A. P., Texeira, V. W. and Teixeira, A. A. C. 2021. Environmental and abiotic factors interfere in *Leptodactylus macrosternum* (Anura, Leptodactylidae) reproduction despite no changes in sexual hormones levels. – Res. Soc. Dev. 10: e46110817627.

Cui, Z., Li, W., Yu, S. and Jin, M. 2022. Similarity analysis of dynamic temperature measurements. – Metrol. Meas. Syst. 29: 283–300.

Cunningham, S. J., Gardner, J. L. and Martin, R. O. 2021. Opportunity costs and the response of birds and mammals to climate warming. – Front. Ecol. Environ. 19: 300–307.

De-Carvalho, C. B., Freitas, E. B., Faria, R. G., Batista, R. C., Batista, C. C., Coelho, W. A. and Bocchiglieri, A. 2008. História natural de *Leptodactylus mystacinus* e *Leptodactylus fuscus* (Anura: Leptodactylidae) no Cerrado do Brasil Central. – Biota Neotrop. 8: 105–115.

Deutsch, C. A., Tewksbury, J. J., Huey, R. B., Sheldon, K. S., Ghalambor, C. K., Haak, D. C. and Martin, P. R. 2008. Impacts of climate warning on terrestrial ectotherms across latitude. – Proc. Natl Acad. Sci. USA 105: 6668–6672.

Díaz-Ricaurte, J. C., Serrano, F. C., Guevara-Molina, E. C., Araujo, C. and Martins, M. 2020. Does behavioral thermal tolerance predict distribution pattern and habitat use in two sympatric Neotropical frogs? – PLoS One 15: e0239485.

Duarte, H., Tejedo, M., Katzenberger, M., Marangoni, F., Baldo, D., Beltrán, J. F., Martí, D. A., Richter-Boix, A. and Gonzalez-Voyer, A. 2012. Can amphibians take the heat? Vulnerability to climate warming in subtropical and temperate larval amphibian communities. – Global Change Biol. 18: 412–421.

Eiter, T. and Mannila, H. 1994. Computing discrete Fréchet distance. Technical Report CD-TR 94/64. – Christian Doppler Laboratory for Expert Systems, Technical Univ. Vienna.

Enriquez-Urzelai, U., Kearney, M. R., Nicieza, A. G. and Tingley, R. 2019. Integrating mechanistic and correlative niche models to unravel range-limiting processes in a temperate amphibian. – Global Change Biol. 25: 2633–2647.

Feder, M. E. and Londos, P. L. 1984. Hydric constraints upon foraging in a terrestrial salamander, *Desmognathus ochrophaeus* (Amphibia: Plethodontidae). – Oecologia 64: 413–418.

Forget-Klein, É. and Green, D. M. 2021. Toads use the subsurface thermal gradient for temperature regulation underground. – J. Therm. Biol. 99: 102956.

Fouquet, A., Gilles, A., Vences, M., Marty, C., Blanc, M. and Gemmell, N. J. 2007. Underestimation of species richness in Neotropical frogs revealed by mtDNA Analyses. – PLoS One 2: e1109.

Ginal, P., Mokhatla, M., Kruger, N., Secondi, J., Herrel, A., Measey, J. and Rödder, D. 2021. Ecophysiological models for global invaders: is Europe a big playground for the African clawed frog? – J. Exp. Zool. A 335: 158–172.

Greenberg, D. A. and Palen, W. J. 2021. Hydrothermal physiology and climate vulnerability in amphibians. – Proc. R. Soc. B 288: 20202273.

Gunderson, A. R. and Leal, M. 2016. A conceptual framework for understanding thermal constraints on ectotherm activity with implications for predicting responses to global change. – Ecol. Lett. 19: 111–120.

Haddad, C. F. D., Toledo, L. F., Prado, C. P. A., Loebmann, D., Gasparini, J. L. and Sazima, I. 2013. Guia dos anfíbios da Mata Atlântica: diversidade e biologia. – Anolisbooks.

Hansen, M. C., Potapov, P. V., Moore, R., Hancher, M., Turubanova, S. A., Tyukavina, A., Thau, D., Stehman, S. V., Goetz,




16000587, 2026, 1, Downloaded from https://nsojournals.onlinelibrary.wiley.com/doi/10.1002/ecog.07617 by Universidade Estadual Paulista, Wiley Online Library on [04/09/2026]. See the Terms and Conditions (https://onlinelibrary.wiley.com/terms-and-conditions) on Wiley Online Library for rules of use; OA articles are governed by the applicable Creative Commons License

S. J., Loveland, T. R., Kommareddy, A., Egorov, A., Chini, L., Justice, C. O. And Townshend, J. R. G. 2013. High resolution global maps of 21st-century forest cover change. – Science 342: 850–853.
Henrique, R. S. and Grant, T. 2019. Influence of environmental factors on short-term movements of butter frogs (*Leptodactylus latrans*). – Herpetologica 75: 38–46.
Hillman, S. S. 1980. Physiological correlates of differential dehydration tolerance in anuran amphibians. – Copeia 1980: 125–129.
Hitchcock, M. A. and McBrayer, L. D. 2006. Thermoregulation in nocturnal ecthotherms: seasonal and intraspecific variation in the Mediterranean gecko (*Hemidactylus turcicus*). – J. Herpetol. 40: 185–195.
Huang, S. P., Kearley, R. E., Hung, K. and Porter, W. P. 2020. Evaporative water loss simulation improves models' prediction of habitat suitability for a high-elevation forest skink. – Oecologia 192: 657–669.
Huey, R. B. and Kingsolver, J. G. 2019. Climate warming, resource availability, and the metabolic meltdown of ectotherms. – Am. Nat. 194: E140–E150.
Huey, R. B. and Slatkin, M. 1976. Cost and benefits of lizard thermoregulation. – Q. Rev. Biol. 51: 363–384.
Huey, R. B. and Stevenson, R. D. 1979. Integrating thermal physiology and ecology of ectotherms: a discussion of approaches. – Am. Zool. 19: 357–366.
Kearney, M., Phillips, B. L., Tracy, C. R., Christian, K. A., Betts, G. and Porter, W. P. 2008. Modelling species distributions without using species distributions: the cane toad in Australia under current and future climates. – Ecography 31: 423–434.
Kearney, M. R. 2013. Activity restriction and the mechanistic basis for extinctions under climate warming. – Ecol. Lett. 16: 1470–1479.
Kearney, M. R., Isaac, A. P. and Porter, W. P. 2014. microclim: global estimates of hourly microclimate based on long-term monthly climate averages. – Sci. Data 1: 140006.
Kearney, M. R. and Porter, W. P. 2017. NicheMapR – an R package for biophysical modelling: the microclimate model. – Ecography 40: 664–674.
Kearney, M. R., Munns, S. L., Moore, D., Malishev, M. and Bull, C. 2018. Field tests of a general ectotherm niche model show how water can limit lizard activity and distribution. – Ecol. Monogr. 88: 672–693.
Köhler, A., Sadowska, J., Olszewska, J., Trzeciak, P., Berger-Tal, O. and Tracy, C. R. 2011. Staying warm or moist? Operative temperature and thermal preferences of common frogs (*Rana temporaria*), and effects on locomotion. – J. Herpetol. 21: 17–26.
Lertzman-Lepofsky, G. F., Kissel, A. M. and, Sinervo, B. 2020. Water loss and temperature interact to compound amphibian vulnerability to climate change. – Global Change Biol. 26: 4868–4879.
Lillywhite, H. B. 2006. Water relations of tetrapod integument. – J. Exp. Biol. 209: 202–226.
Lucas, E. M., Brasileiro, C. A., Oyamaguchi, H. M. and Martins, M. 2008. The reproductive ecology of *Leptodactylus fuscus* (Anura, Leptodactylidae): new data from natural temporary ponds in the Brazilian Cerrado and a review throughout its distribution. – J. Nat. Hist. 42: 2305–2320.
Maenaka, B. M., Senzano, L. M. and Andrade, D. V. 2023. Seasonal variation in thermal biology and water balance in a year-round active Neotropical treefrog, *Scinax fuscovarius*. – Herpetologica 79: 155–165.
Maffei, F., Ubaid, F. K. and Jim, J. 2011. Anurans in an open cerrado area in the municipality of Borebi, São Paulo state, southeastern Brazil: habitat use, abundance and seasonal variation. – Biota Neotrop. 11: 221–233.
Magalhães, F. M., Lyra, M. L., de Carvalho, T. R., Baldo, D., Brusquetti, F., Burella, P., Colli, G. R., Gehara, M. C., Giaretta, A. A., Haddad, C. F. B., Langone, J. A., López, J. A., Napoli, M. F., Santana, D. J., de Sá, R. O. and Garda, A. A. 2020. Taxonomic review of South American butter frogs: phylogeny, geographic patterns, and species delimitation in the *Leptodactylus latrans* species group (Anura: Leptodactylidae). – Herpetol. Monogr. 34: 131–177.
Marsh, C. J., Syfert, M. M., Aletrari, E., Gavish, Y., Kunin, W. E. and Brummitt, N. 2023. The effect of sampling effort and methodology on range size estimates of poorlyrecorded species for IUCN Red List assessments. – Biodivers. Conserv. 32: 1105–1123.
Martins, M. 1988. Biologia reprodutiva de *Leptodactylus fuscus* em Boa Vista, Roraima (Amphibia: Anura). – Rev. Bras. Biol. 48: 969–977.
Méndez-Narváez, J., Flechas, S. V. and Amézquita, A. 2015. Foam nests provide context-dependent thermal insulation to embryos of three Leptodactylid frogs. – Physiol. Biochem. Zool. 88: 246–253.
Mitchell, A. and Bergmann, P. J. 2016. Thermal and habitat preferences do not maximize jumping performance in frogs. – Funct. Ecol. 30: 733–742.
Muñoz, M. M. and Bodensteiner, B. L. 2019. Janzen's hypothesis meets the Bogert effect: connecting climate variation, thermoregulatory behavior, and rates of physiological evolution. – Integr. Org. Biol. 1: 1–12.
Nowakowski, A. J., Watling, J. I., Whitfield, S. M., Todd, B. D., Kurz, D. J. and Donnelly, M. A. 2017. Tropical amphibians in shifting thermal landscapes under land-use and climate change. – Conserv. Biol. 31: 96–105.
O'Connor, M. P. and Tracy, C. R. 1992. Thermoregulation by juvenile toads of *Bufo woodhousei* in the field and in the laboratory. – Copeia 1992: 865–876.
Oliveira-Filho, J. C. and Giaretta, A. A. 2008. Reproductive behavior of *Leptodactylus mystacinus* (Anura, Leptodactylidae) with notes on courtship call of other *Leptodactylus* species. – Iheringia ser. Zool. 98: 508–515.
Oromí, N., Sanuy, D. and Sinsch, U. 2010. Thermal ecology of natterjack toads (*Bufo calamita*) in a semiarid landscape. – J. Therm. Biol. 35: 34–40.
Ortega-Chinchilla, J. E., Cabanzo-Olarte, L. C., Vaz, R., Lamadrid-Feris, F., Bevier, C. R. and Navas, C. A. 2022. Behavioral models of hydrothermal regulation in anurans: a field study in the Atlantic Forest, Brazil. – Biotropica 55: 329–338.
Pearson, R. G., Raxworthy, C. J., Nakamura, M. and Peterson, A. T. 2007. Predicting species distributions from small numbers of occurrence records: a test case using cryptic geckos in Madagascar. – J. Biogeogr. 34: 102–117.
Pena, J. C. C., Kamino, L. H. Y., Rodriguez, M., Mariano-Neto, E. and Siqueira, M. F. 2014. Assessing the conservation status of species with limited available data and disjunct distribution. – Biol. Conserv. 170: 130–136.
Peterman, W. E. and Semlitsch, R. D. 2014. Spatial variation in water loss predicts terrestrial salamander distribution and population dynamics. – Oecologia 176: 357–369.
Peterson, A. T. and Raghavan, R. K. 2017. The geographic distribution of *Ixodes scapularis* (Acari: Ixodidae) revisited: the impor-



16000587, 2026, 1, Downloaded from https://nsojournals.onlinelibrary.wiley.com/doi/10.1002/ecog.07617 by Universidade Estadual Paulista, Wiley Online Library on [04/09/2026]. See the Terms and Conditions (https://onlinelibrary.wiley.com/terms-and-conditions) on Wiley Online Library for rules of use; OA articles are governed by the applicable Creative Commons License

tance of assumptions about error balance. – J. Med. Entomol. 54: 1080–1084.
Porter, W. P., Mitchell, J. W., Beckman, W. A. and DeWitt, C. B. 1973. Behavioral implications of mechanistic ecology. – Oecologia 13: 1–54.
Prado, C. P. A., Uetanabaro, M. and Lopes, F. S. 2000. Reproductive strategies of *Leptodactylus chaquensis* and *L. podicipinus* in the Pantanal, Brazil. – J. Herpetol. 34: 135–139.
Rezende, E. L., Castañeda, L. E. and Santos, M. 2014. Tolerance landscapes in thermal ecology. – Funct. Ecol. 28: 799–809.
Riddell, E. A., Apanovitch, E. K., Odom, J. P. and Sears, M. W. 2017. Physical calculations of resistance to water loss improve predictions of species range models. – Ecol. Monogr. 87: 21–33.
Rittenhouse, T. A. G., Harper, E. B., Rehard, L. R. and Semlitsch, R. D. 2008. The role of microhabitats in the desiccation and survival of anurans in recently harvested oak–hickory forest. – Copeia 2008: 807–814.
Rock, J. and Cree, A. 2008. Extreme variation in body temperature in a nocturnal thigmothermic lizard. – J. Herpetol. 18: 69–76.
Rozen-Rechels, D., Dupoué, A., Lourdais, O., Chamaillé, S., Meylan, S., Clobert, J. and Le Galliard, J. 2019. When water interacts with temperature: ecological and evolutionary implications of thermo-hydroregulation in terrestrial ectotherms. – Ecol. Evol. 9: 10029–10043.
Rozen-Rechels, D., Farigoule, P., Agostini, S., Badiane, A., Meylan, S. and Le Galliard, J. F. 2020. Short-term change in water availability influences thermoregulation behaviours in a dry-skinned ectotherm. – J. Anim. Ecol. 89: 2099–2110.
Rubalcaba, J. G., Gouveia, S. F. and Ollaga-Tárraga, M. A. 2019a. A mechanistic model to scale up biophysical processes into geographical size gradients in ectotherms. – Global Ecol. Biogeogr. 28: 793–803.
Rubalcaba, J. G., Gouveia, S. F. and Olalla-Tárraga, M. A. 2019b. Upscaling microclimatic conditions into body temperature distributions of ectotherms. – Am. Nat. 193: 677–687.
Ruthsatz, K., Rakotoarison, A., Razafimampiandra, J., Randriamahefa, V. S., Rabemananjara, F., Rakotondraparany, F., Bletz, M. C. and Vences, M. 2022. Field body temperatures in Malagasy rainforest frogs. – Herpetol. Notes 15: 565–578.
Sá, R. O., Grant, T., Camargo, A., Heyer, W. R., Ponssa, M. L. and Stanley, E. 2014. Systematics of the Neotropical genus *Leptodactylus* Fitzinger, 1826 (Anura: Leptodactylidae): phylogeny, the relevance of non-molecular evidence, and species accounts. – S. Am. J. Herpetol. 9: S1–S100.
Scheffers, B. R., Brunner, R. M., Ramirez, S. D., Shoo, L. P., Diesmos, A. and Williams, S. E. 2013. Thermal buffering of microhabitats is a critical factor mediating warming vulnerability of frogs in the Philippine biodiversity hotspot. – Biotropica 45: 628–635.
Schwarzkopf, L. and Alford, R. A. 1996. Desiccation and shelter-site use in a tropical amphibian: comparing toads with physical models. – Funct. Ecol. 10: 193–200.
Sears, M. W., Angilletta, M. J., Schuler, M. S., Borchert, J., Dilliplane, K. F., Stegman, M., Rusch, T. W. and Mitchell, W. A. 2016. Configuration of the thermal landscape determines thermoregulatory performance of ectotherms. – Proc. Natl Acad. Sci. USA 113: 10595–10600.
Seebacher, F. and Alford, W. A. 2002. Shelter microhabitats determine body temperature and dehydration rates of a terrestrial amphibian (*Bufo marinus*). – J. Herpetol. 36: 69–75.
Senzano, L. M., Ribeiro, M. C., Gouveia, S. F. and Andrade, D. V. 2025. Data from: Combining thermal and hydric constraints for spatially predicting the activity suitability of Neotropical leptodactylid frogs. – Dryad Digital Repository, https://doi.org/10.5061/dryad.02v6wwqhg.
Silva, J. P. N. 2016. Composição e distribuição de anfíbios anuros em poças temporárias em área de Caatinga no município de Cuité-PB. – BSc thesis, Universidade Federal de Campina Grande, Paraíba, Brazil.
Silva, W. R. and Giaretta, A. A. 2008. Further notes on the natural history of the South American pepper frog, *Leptodactylus labyrinthicus* (Spix, 1824) (Anura, Leptodactylidae). – Braz. J. Biol. 68: 403–407.
Simioni, F., Campos, V. A., Dorado-Rodrigues, T. F., Penha, J. and Strüssmann, C. 2014. Crab burrows and termite thermal chimneys as refuges for anurans in a Neotropical wetland. – Salamandra 50: 133–138.
Simon, M. N., Ribeiro, P. L. and Navas, C. A. 2015. Upper thermal tolerance plasticity in tropical amphibian species from contrasting habitats: implications for warming impact prediction. – J. Therm. Biol. 48: 36–44.
Sinervo, B. et al. 2010. Erosion of lizard diversity by climate change and altered thermal niches. – Science 328: 894–899.
Smits, A. W. 1984. Activity patterns and thermal biology of the toad *Bufo boreas halophilus*. – Copeia 3: 689–696.
Solano, H. 1987. Algunos aspectos de la biología reproductiva del sapito silvador *Leptodactylus fuscus* (Schneider) (Amphibia: Leptodactylidae). – Amphib. Reptilia 8: 111–128.
Sunday, J. M., Bates, A. E., Kearney, M. R., Colwell, R. K., Dulvy, N. K., Longino, J. T. and Huey, R. B. 2014. Thermal-safety margins and the necessity of thermoregulatory behavior across latitude and elevation. – Proc. Natl Acad. Sci. USA 111: 5610–5615.
Syfert, M. M., Joppa, L., Smith, M. J., Coomes, D. A., Bachman, A. P. and Brummitt, N. A. 2014. Using species distribution models to inform IUCN Red List assessments. – Biol. Conserv. 177: 174–184.
Tracy, C. R., Tixier, T., Nöene, C. L. and Christian, K. A. 2014. Field hydration state varies among tropical frog species with different habitat use. – Physiol. Biochem. Zool. 87: 197–202.
Venturelli, D. P., Silva, V. R. and Giaretta, A. A. 2021. Tadpoles' resistance to desiccation in species of *Leptodactylus* (Anura, Leptodactylidae). – J. Herpetol. 55: 265–270.
Vieira, W. L. S., Arzabe, C. and Santana, G. G. 2007. Composição e distribuição espaço-temporal de anuros no Cariri paraibano, Nordeste do Brasil. – Oeco. Bras. 11: 383–396.
Wells, K. D. 2007. The ecology and behavior of amphibians. – Univ. Chicago Press.
Woolbright, L. L. 1985. Patterns of nocturnal movement and calling by the tropical frog *Eleutherodactylus coqui*. – Herpetology 41: 1–9.
Zina, J. and Haddad, C. F. B. 2005. Reproductive activity and vocalizations of *Leptodactylus labyrinthicus* (Anura: Leptodactylidae) in southern Brazil. – Biota Neotrop. 5: BN00605022005.



16000587, 2026, 1, Downloaded from https://nsojournals.onlinelibrary.wiley.com/doi/10.1002/ecog.07617 by Universidade Estadual Paulista, Wiley Online Library on [04/09/2026]. See the Terms and Conditions (https://onlinelibrary.wiley.com/terms-and-conditions) on Wiley Online Library for rules of use; OA articles are governed by the applicable Creative Commons License